THE JOURNAL OF BIOLOGICAL CHEMISTRY VOL. 290, NO. 31, pp. 19146–19157, July 31, 2015

Insulin Resistance Prevents AMPK-induced Tau Dephosphorylation through Akt-mediated Increase in AMPK$^{Ser\text{-}485}$ Phosphorylation*

Received for publication, January 6, 2015, and in revised form, June 19, 2015 Published, JBC Papers in Press, June 22, 2015, DOI 10.1074/jbc.M115.636852

Bhumsoo Kim[1], **Claudia Figueroa-Romero, Crystal Pacut, Carey Backus, and Eva L. Feldman**

From the Department of Neurology, University of Michigan, Ann Arbor, Michigan 48109

Background: Insulin resistance is a risk factor for Alzheimer disease.
Results: AMPK$^{Ser\text{-}485}$ is responsible for AMPK-mediated Tau phosphorylation.
Conclusion: Abnormal phosphorylation of AMPK$^{Ser\text{-}485}$ may be the link for the increased Alzheimer disease risk in metabolic syndrome
Significance: With the rapid increase in both metabolic syndrome and Alzheimer disease, it is crucial to understand the underling mechanism linking two diseases

Metabolic syndrome (MetS) is a cluster of cardiovascular risk factors including obesity, diabetes, and dyslipidemia, and insulin resistance (IR) is the central feature of MetS. Recent studies suggest that MetS is a risk factor for Alzheimer disease (AD). AMP-activated kinase (AMPK) is an evolutionarily conserved fuel-sensing enzyme and a key player in regulating energy metabolism. In this report, we examined the role of IR on the regulation of AMPK phosphorylation and AMPK-mediated Tau phosphorylation. We found that AMPK$^{Ser\text{-}485}$, but not AMPK$^{Thr\text{-}172}$, phosphorylation is increased in the cortex of db/db and high fat diet-fed obese mice, two mouse models of IR. *In vitro*, treatment of human cortical stem cell line (HK-5320) and primary mouse embryonic cortical neurons with the AMPK activator, 5-aminoimidazole-4-carboxamide 1-β-D-ribofuranoside (AICAR), induced AMPK phosphorylation at both Thr-172 and Ser-485. AMPK activation also triggered Tau dephosphorylation. When IR was mimicked *in vitro* by chronically treating the cells with insulin, AICAR specifically induced AMPK$^{Ser\text{-}485}$, but not AMPK$^{Thr\text{-}172}$, hyperphosphorylation whereas AICAR-induced Tau dephosphorylation was inhibited. IR also resulted in the overactivation of Akt by AICAR treatment; however, preventing Akt overactivation during IR prevented AMPK$^{Ser\text{-}485}$ hyperphosphorylation and restored AMPK-mediated Tau dephosphorylation. Transfection of AMPK^{S485A} mutant caused similar results. Therefore, our results suggest the following mechanism for the adverse effect of IR on AD pathology: IR → chronic overactivation of Akt → AMPK$^{Ser\text{-}485}$ hyperphosphorylation → inhibition of AMPK-mediated Tau dephosphorylation. Together, our results show for the first time a possible contribution of IR-induced AMPK$^{Ser\text{-}485}$ phosphorylation to the increased risk of AD in obesity and diabetes.

Alzheimer disease (AD)[2] is a progressive neurodegenerative disease characterized by loss of memory and other cognitive functions necessary to perform complex daily activities (1). The most prominent neuropathological features of AD are the appearance of senile plaques composed of amyloid β peptides and neurofibrillary tangles derived from the aggregation of the microtubule-associated protein Tau (2, 3). AD is the most common form of dementia, accounting for over 70% of all cases, and it currently affects 5.4 million Americans. The incidence is expected to reach over 13.8 million by 2050, and it is estimated that the cost for caring for people with AD will dramatically increase from $203 billion for 2013 to $1.2 trillion by 2050.

Insulin resistance (IR) is defined as a state of reduced responsiveness of target tissue(s) to normal circulating levels of insulin. It is the central feature of metabolic syndrome (MetS), a constellation of disorders related to an increased risk of cardiovascular disease, and it is the major contributor for the development of diabetes (4). Multiple studies report that patients with MetS have an increased risk of developing AD compared with age- and gender-matched controls (5). In addition, accumulating evidence suggests that AD is closely related to dysfunction of both insulin signaling and glucose metabolism in the brain, prompting some investigators to refer to AD as type 3 diabetes or an insulin-resistant brain state (6, 7). Epidemiological studies also demonstrate an association between obesity caused by caused by dietary fat intake and an increased risk for AD (8), and multiple studies report that patients with diabetes have a 50–75% increased risk of developing AD compared with age- and gender-matched control groups (9–13). In parallel, a study of the Mayo Clinic AD Patient Registry revealed that 80% of AD patients have either type 2 diabetes or impaired fasting glucose (14).

There are many theories to explain the connection between AD and diabetes (and MetS in general), including impaired

* This work was supported, in whole or in part, by National Institutes of Health Grants 1DP3DK094292 and 1R24082841 (to E. L. F.). This work was also supported by the Program for Neurology Research and Discovery. The authors declare that they have no conflicts of interest with the contents of this article.

[1] To whom correspondence should be addressed: Univ. of Michigan Dept. of Neurology, 109 Zina Pitcher Place, 5371 AAT-BSRB, Ann Arbor, MI 48109. Tel.: 734-763-7274; Fax: 734-763-7275; E-mail: bhumsoo@umich.edu.

[2] The abbreviations used are: AD, Alzheimer disease; IR, insulin resistance; MetS, metabolic syndrome; AMPK, AMP-activated kinase; HFD, high fat diet; NSDM, neural stem differentiation media; AICR, 5-aminoimidazole-4-carboxamide 1-β-D-ribofuranoside.

brain insulin signaling and the resulting IR (15, 16), mitochondrial dysfunction (17, 18), and disturbance in lipid and cholesterol metabolism (19). One theory suggests perturbed brain energy metabolism as the cause of pathogenic development of AD and cognitive impairment in general (20). Disruption in energy metabolism increases IR, affects glucose metabolism, and causes mitochondrial dysfunction, all of which are risk factors for AD (21). AMP-activated protein kinase (AMPK) is an evolutionarily conserved fuel-sensing enzyme and a key player in regulating energy metabolism (22). AMPK is activated during energy shortages and suppressed in energy surplus by sensing cellular AMP/ATP ratios. AMPK functions to restore cellular energy metabolism by suppressing energy consuming anabolic pathways and stimulating catabolic energy producing pathways (23).

In AD, the role of AMPK is controversial, with the reports suggesting both beneficial and detrimental effects on the progression of AD (20). It is reported that AMPK activation reduces amyloid β production in rat cortical neurons (24) and that leptin and resveratrol reduce amyloid β levels and Tau phosphorylation through AMPK activation (25–27). In contrast, AMPK can directly phosphorylate Tau, and amyloid β-induced increases in Tau phosphorylation require AMPK-activated Ca^{2+}/calmodulin-dependent protein kinase kinase β (28). Furthermore, increased AMPK activation is observed in tangle- and pretangle-bearing neurons in AD brain (29). This activation of AMPK requires phosphorylation at threonine 172 (AMPK$^{Thr-172}$), a residue in its α-subunit, by upstream kinases such as liver kinase B1 (LKB1) or Ca^{2+}/calmodulin-dependent protein kinase kinase β (21, 30). AMPK is also phosphorylated at serine 485 (AMPK$^{Ser-485}$) by Akt, which reduces Thr-172 phosphorylation and inhibits AMPK activation (31, 32); however, the direct contribution of Ser-485 on AMPK activation has not been extensively studied.

In this study, we report a novel role of AMPK$^{Ser-485}$ on Tau phosphorylation. We demonstrate that AMPK$^{Ser-485}$, but not AMPK$^{Thr-172}$, phosphorylation is increased in two animal models of diabetes and obesity. Our results also indicate that activation of AMPK by the AMPK activator AICAR decreases Tau phosphorylation and that this change is specifically correlated with changes in AMPK$^{Ser-485}$ phosphorylation. Finally, we demonstrate that Akt hyperactivation caused by IR may be responsible for the increased AMPK$^{Ser-485}$ phosphorylation and subsequent inhibition of AICAR-mediated Tau dephosphorylation. These results show for the first time how AMPK$^{Ser-485}$ phosphorylation may contribute to the increased risk of AD in obesity and diabetes.

Experimental Procedures

Antibodies and Chemicals—Polyclonal antibodies against phosphorylated Tau (Ser(P)-199/202, Ser(P)-262, Ser(P)-396, and Thr(P)-231) were purchased from Life Technologies Inc. Tau1 (recognizing dephosphorylated Tau), Tau5 (for total Tau), and anti-GAPDH antibodies were from Millipore (Billerica, MA). LY294002 and U0126 were also from Millipore. Ser(P)-485-AMPK and actin antibodies were from Abcam (Cambridge, MA). The antibodies for Thr(P)-172-AMPK, and AMPK were purchased from Cell Signaling (Beverly, MA).

TABLE 1
Diet composition

	D12450B		D05090701	
	gm	kcal	gm	kcal
Product				
Protein	19	20	25	20
Carbohydrate	67	70	32	26
Fat	4	10	30	54
Total		100		100
kcal/gm	3.85		5.04	
Ingredient				
Casein, 80 mesh	200	800	200	800
L-Cystein	3	12	3	12
Corn starch	315	1260	56.3	225
Maltodextrin 10	35	140	125	500
Sucrose	350	1400	68.8	275
Cellulose, BW200	50	0	50	0
Soybean oil	25	225	25	225
Lard	20	180	220	1980
Mineal mix S10026	10	0	10	0
Dicalcium phosphate	13	0	13	0
Calcium carbonate	5.5	0	5.5	0
Potassium citrate, 1 H_2O	16.5	0	16.5	0
Vitamin mix V10001	10	10	10	40
Choline bitartrate	2	0	2	0
FD&C yellow dye #5	0.05	0	0.025	0
FD&C red dye #40	0	0	0.025	0
FD&C blue dye #1	0	0	0	0
Total	1055.05	4057	805.15	4057

AICAR was purchased from Sigma-Aldrich. All other chemicals were purchased from either Sigma-Aldrich or Fisher Scientific (Fair Lawn, NJ).

Mouse Models and Brain Preparation—BKS-db/db and db^{+} (BKS.Cg-m$^{+/+}$ Lepr^{db}/J, JAX mice stock #000642) mice were purchased from Jackson Laboratory (Bar Harbor, ME). C57BL6 (B6) mice, a commonly used model to study diet-induced obesity (20, 21, 22, 23), were also from Jackson Laboratory. Obesity was induced in B6 mice by placing them on a high fat diet (HFD) consisting of 54% kcal from fat (D05090701; Research Diets Inc., New Brunswick, NJ;) at 4 weeks of age until 24 weeks of age, whereas control mice were fed a standard diet consisting of 10% kcal from fat (D12450B; Research Diets Inc.) (Table 1). Fasting blood glucose levels were measured every 4 weeks using a standard glucometer (OneTouch; LifeScan Inc., Milpitas, CA). All mice were housed in a pathogen-free environment and cared for following the University of Michigan Committee on the Care and Use of Animals guidelines.

Mice were euthanized per our published protocols with an overdose of sodium pentobarbital (33, 34). For Western immunoblotting analyses, brains were cut in half, the cortex and hippocampus were separated, and then tissues were snap frozen in liquid nitrogen and stored at −80 °C until use. At least six animals were analyzed for each treatment, and three or four representative Western blotting results are shown on each figure.

Cell Culture and Treatments—HK-532 human cortical stem cells were provided by Neuralstem, Inc. (Rockville, MD). Cells were incubated in differentiation medium (NSDM) for 7–10 days, and the medium was changed to NSDM without insulin 24 h before treatment.

Primary cortical neurons were prepared from embryonic day 15 embryos of Sprague-Dawley rats. Cells were maintained in feed medium (neurobasal media; Invitrogen) supplemented with B27 without antioxidant (Invitrogen) and other supple-

ments as described previously (35) for 6 days before being used in experiments. Culture medium was changed to treatment medium (feed medium without B27 and antibiotics) 18 h before insulin and/or AICAR treatments.

Construction, Production, and Infection of Lentiviral Expression Vectors—Human AMPKa1 cDNA was amplified from SH-SY5Y human neuroblastoma cell cDNA and directionally subcloned into the XhoI and NotI sites of the lentiviral expression vector pLVX-IRES-mCherry (Clontech). The S485A and S485D mutants of AMPK were created by the QuikChange method (Stratagene, La Jolla, CA). All constructs were confirmed by sequencing. Lentiviral stocks were generated by the University of Michigan Vector Core. HK-532 cells were infected with 10× viral stock 3 days into differentiation for 6 h. The cells were harvested 5 days after infection following insulin and/or AMPK treatment as described in the results. For the generation of the stable clones, cells were selected by puromycin resistance.

Western Immunoblotting—Western immunoblotting was performed as described previously (35). Mouse cortex was homogenized using a plastic pestle in a microcentrifuge tube in T-PER tissue protein extraction reagent (Pierce) with a protease inhibitor tablet. Samples were briefly sonicated and centrifuged at 13,000 rpm for 20 min at 4 °C, and supernatants were collected. Cultured cells were lysed in radioimmune precipitation assay buffer (Pierce) with protease inhibitor mixture (Roche Diagnostics, Indianapolis, IN). Lysates were collected, briefly sonicated, and centrifuged at 13,000 rpm for 15 min at 4 °C prior to the collection of supernatants. Protein concentration of the brain and cortical neuron lysates were measured with the Pierce 660-nm protein assay reagent (Thermo Scientific, Rockford, IL). The lysates were separated by SDS-PAGE and transferred to nitrocellulose membranes. After blocking with 3% BSA in TBS with 0.1% Tween 20, nitrocellulose membranes were incubated with the appropriate primary antibodies at 4 °C overnight followed by secondary antibodies conjugated with horseradish peroxidase (Santa Cruz) at room temperature for 2 h. Signals were visualized using enhanced chemiluminescence reagents (ECL; Amersham Bioscience) or SuperSignal West Femto maximum sensitivity substrate (Pierce), depending on the signal strength. Images were captured using the Chemidoc XRS system and analyzed by Quantity One software (Bio-Rad). In some experiments, the nitrocellulose membranes were incubated at 60 °C for 15 min in stripping solution (2% SDS, 100 mM dithiothreitol, and 100 mM Tris, pH 6.8) and then utilized for immunoblotting with an additional antibody. All experiments were repeated at least three times, and representative results are presented in the figures.

Statistical Analysis—At least six animals were used for statistical analysis for *in vivo* experiments. All *in vitro* experiments were repeated at least three times and presented as the means ± S.E. Statistical analysis was performed by either one-way analysis of variance with Tukey's postanalysis or Student's *t* test depending on the number of comparison groups, using GraphPad Prism software (GraphPad Software Inc., San Diego, CA). Statistical significance was defined as $p < 0.05$.

Results

db/db mice demonstrates an elevation of plasma insulin at ~2 weeks and of blood sugar at 4–6 weeks. By 8 weeks of age, hyperinsulinemia and hyperglycemia were stable phenotypes of the db/db mice (36). At 24 weeks, db/db mice display the full blown diabetes phenotypes with the increased body weight and blood glucose and glycated hemoglobulin (Fig. 1*A*). However, as the diabetic phenotype continues to deteriorate the mice prone to a spontaneous death, so we harvested the mice at 24 weeks. Mice fed with high fat diet usually display signs of prediabetes starting around 16 weeks of age (37, 38). Their blood glucose level and body weight continue to increase up to a year (39). We observed that HFD mice display increased body weight (Fig. 1*A*) and impaired glucose tolerance test (Fig. 1*B*) but no significant changes in blood glucose and glycated hemoglobulin levels indicating that they are prediabetic.

AMPK is an evolutionarily conserved serine/threonine kinase that plays a pivotal role in maintaining cellular homeostasis (22); therefore, we first examined the changes in AMPK phosphorylation in the brain of two IR mouse models; diabetic mice (db/db) or obese mice (HFD-fed). AMPK phosphorylation at Thr-172 in the cortex of db/db mice was not significantly different from that in control db+ mice (Fig. 2*A*). Similarly, mice fed a HFD for 24 weeks did not affect AMPK$^{Thr-172}$ phosphorylation in the cortex (Fig. 2*B*). In contrast, however, AMPK$^{Ser-485}$ was significantly increased in both db/db (2-fold) and obese (1.7-fold) mouse cortices compared with control animals (Fig. 2, *A* and *B*). In addition, Tau phosphorylation was increased in HFD mouse cortex compared with controls (Fig. 2*C*). Increased Ser/Thr phosphorylation of IRS proteins is one of the key features of IR (40). We observed consistently increased IRS phosphorylation (Fig. 2*D*). Basal phosphorylation of Akt was also increased in HFD mouse cortex; the increase in ERK phosphorylation was less significant compared with control animals. We previously reported similar changes in Tau phosphorylation as well as insulin signaling components in db/db mouse brains (36). These results imply that MetS factors, such as diabetes and obesity, may underlie the observed changes in AMPK and Tau phosphorylation.

To examine the role of AMPK on Tau phosphorylation in more detail, we used *in vitro* cell culture models utilizing HK-532 cortical stem cells and primary rat cortical neurons. Treatment of HK-532 cells with the AMPK activator, AICAR, resulted in time- and concentration-dependent increases in AMPK phosphorylation at both Thr-172 and Ser-485 (Fig. 3*A*). AMPK phosphorylation was maintained at least 6 h after AICAR treatment. Because of serine and threonine phosphorylation, total AMPK immunoblotting resulted in a diffuse pattern. Acetyl-CoA carboxylase phosphorylation by AMPK at Ser-79, a surrogate marker for AMPK activation (41), was also increased following AICAR treatment in a manner that corresponded to the observed AMPK phosphorylation (Fig. 3*A*). In parallel, AMPK activation following treatment of HK-532 cells with AICAR for 2 h reduced Tau phosphorylation at Ser-199/202, Thr-231, and Ser-396 (Fig. 3*B*). Tau1 immunoreactivity is also increased after AICAR treatment (Fig. 3*B*), consistent with the prefer-

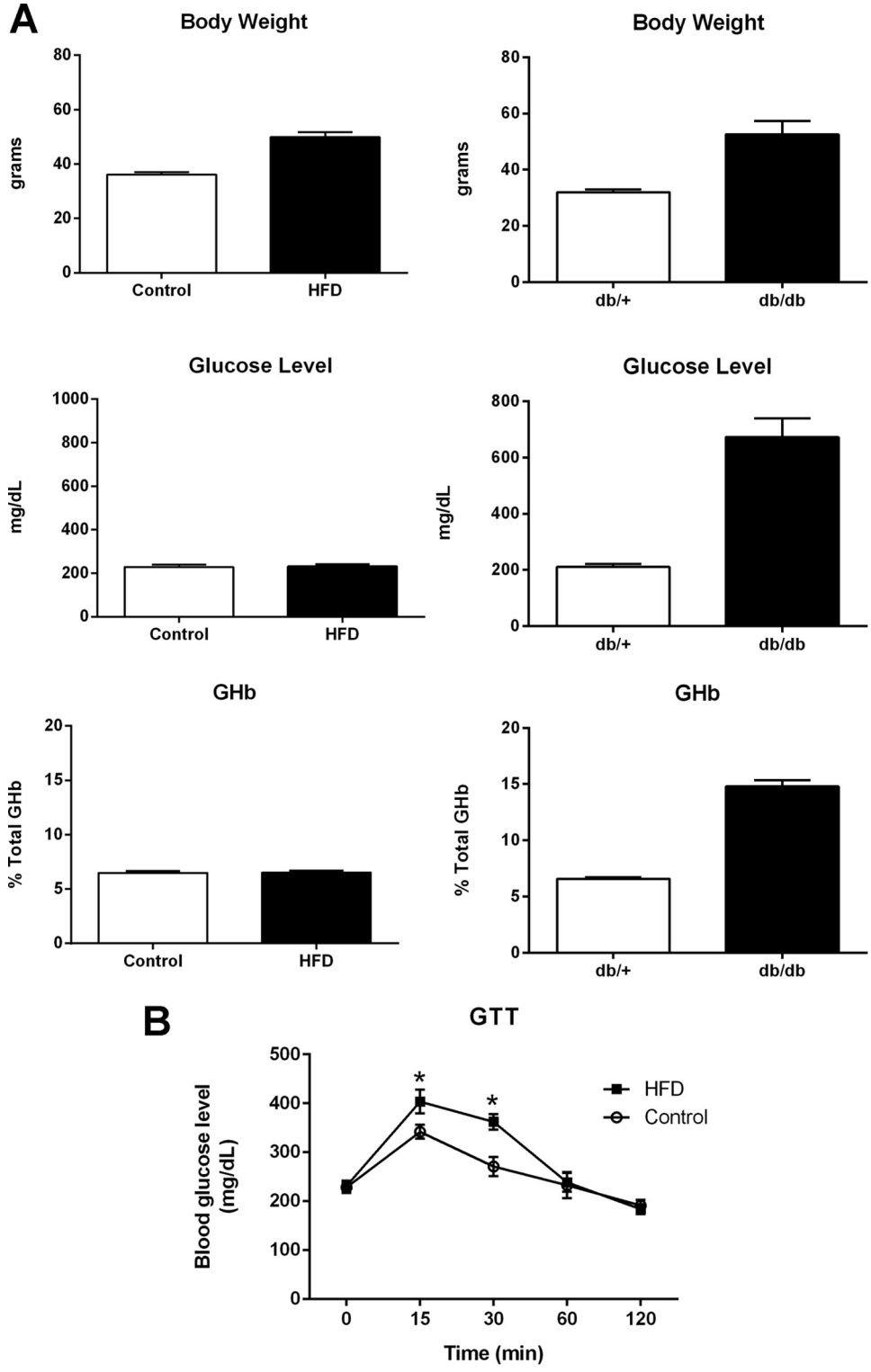

FIGURE 1. **Metabolic phenotyping of db/db and HFD-fed mice.** *A*, body weight, blood glucose, and glycated hemoglobulin (*GHb*) of 24-week-old db/db (*left panels*) mice and mice fed with HFD for 20 weeks (*right panels*). *B*, HFD mice display impaired glucose tolerance test (*GTT*). At least six mice were used for each group. *, $p < 0.05$ by *t* test

ential reaction of the Tau1 antibody with Tau when it is dephosphorylated at serines 195, 198, 199, and 202 (42). Similar changes in AMPK and Tau phosphorylation were observed in primary cortical neurons by AICAR treatment (Fig. 3*C*).

IR is at the core of MetS (4); therefore, we next tested the effect of IR on AMPK-mediated Tau dephosphorylation utilizing HK-532 cortical stem cells and primary rat cortical neurons. We previously reported that chronic insulin treatment of dorsal root ganglia and primary cortical neurons results in a blunted

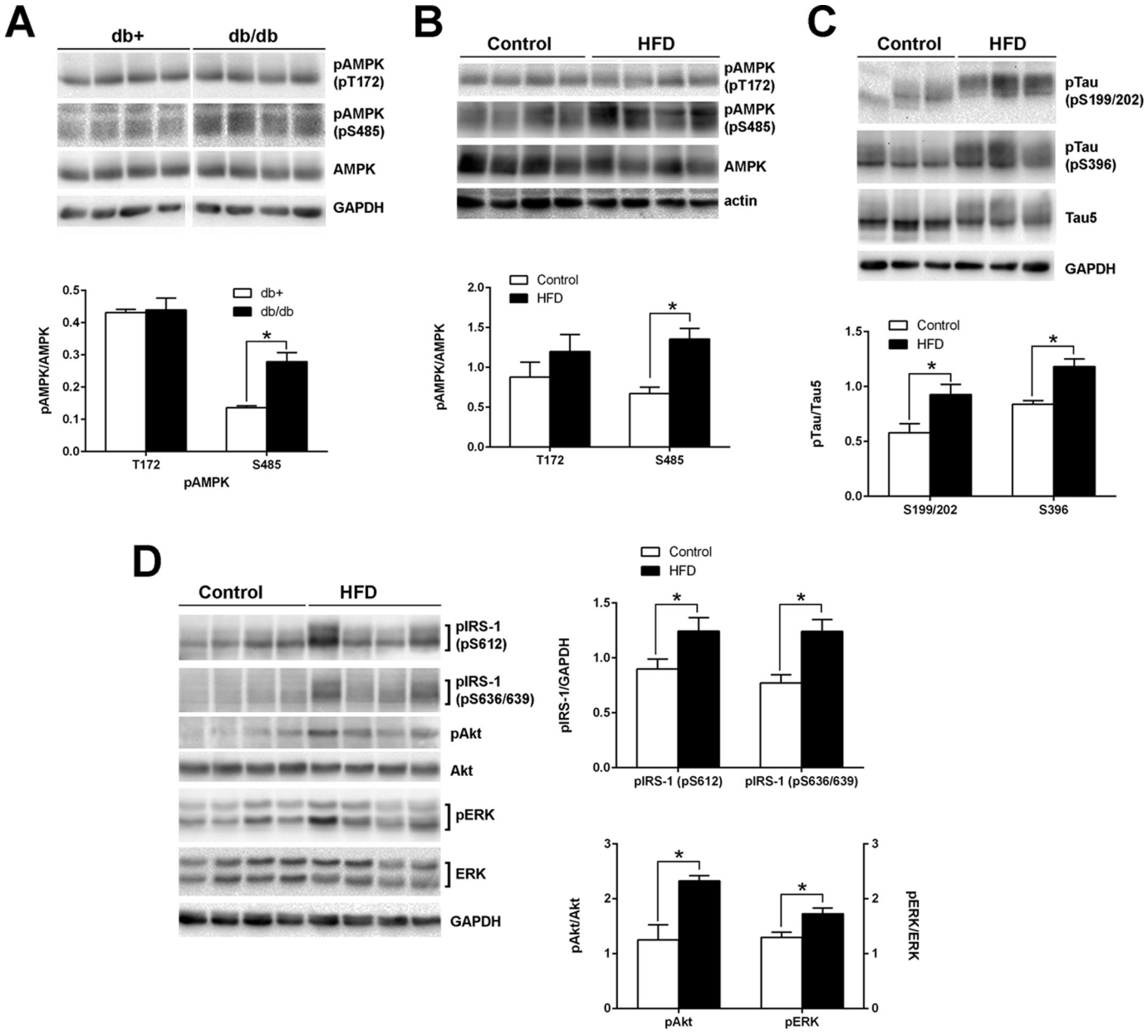

FIGURE 2. **Increased AMPK$^{Ser-485}$ and Tau phosphorylation in db/db and HFD mouse brains.** Cortex from 24-week-old db/db (*A*) or 20-week-old HFD (*B–D*) mouse were homogenized in TPER buffer. The lysates were immunoblotted with the indicated antibodies. The relative density of phosphorylated AMPK over total AMPK (*A* and *B*) and phosphorylated Tau (*pTau*) over total Tau (*Tau5*) (*C*) from the same mouse was measured after immunoblotting. Phosphorylation of IRS-1, Akt, and ERK, the important signaling components of insulin signaling, was also examined from control and HFD cortex (*D*). The results are means ± S.E. of at least six animals per group, and the representative blots are shown. *, $p < 0.05$ by *t* test.

insulin response, suggesting that these models are an excellent means to study neuronal IR *in vitro* (43, 44). To examine the effect of IR on AMPK phosphorylation, we treated HK-532 cells without or with 50 nM insulin overnight and then with 1 mM AICAR for 0, 2, or 6 h. The increase in AMPK$^{Thr-172}$ phosphorylation by AICAR was not significantly different with or without insulin pretreatment (Fig. 4, *A* and *B*, *upper panel*); however, interestingly, AICAR-induced AMPK$^{Ser-485}$ phosphorylation was significantly higher after insulin pretreatment (Fig. 4, *A* and *B*, *lower panel*). As expected, AICAR treatment resulted in Tau dephosphorylation, and induction of IR by chronic insulin treatment prevented AICAR-induced Tau dephosphorylation (Fig. 4, *C* and *D*). We also observed a similar inhibitory effect of IR on AICAR-induced Tau dephosphorylation in embryonic cortical neurons (Fig. 4*E*). Together, these results suggest a connection between increased AMPK$^{Ser-485}$ phosphorylation and Tau phosphorylation, which is abolished in the setting of IR.

To examine the possible mechanism behind IR-mediated changes in AMPK and Tau phosphorylation, we next looked at the contribution of insulin signaling pathway components. To first confirm that the cells are insulin-responsive, we treated HK-532 cells with insulin and observed an increase in Akt phosphorylation, as well as a slight increase in ERK phosphorylation (Fig. 5*A*). It is reported that Akt is the kinase responsible for AMPK$^{Ser-485}$ phosphorylation and the subsequent inhibition of

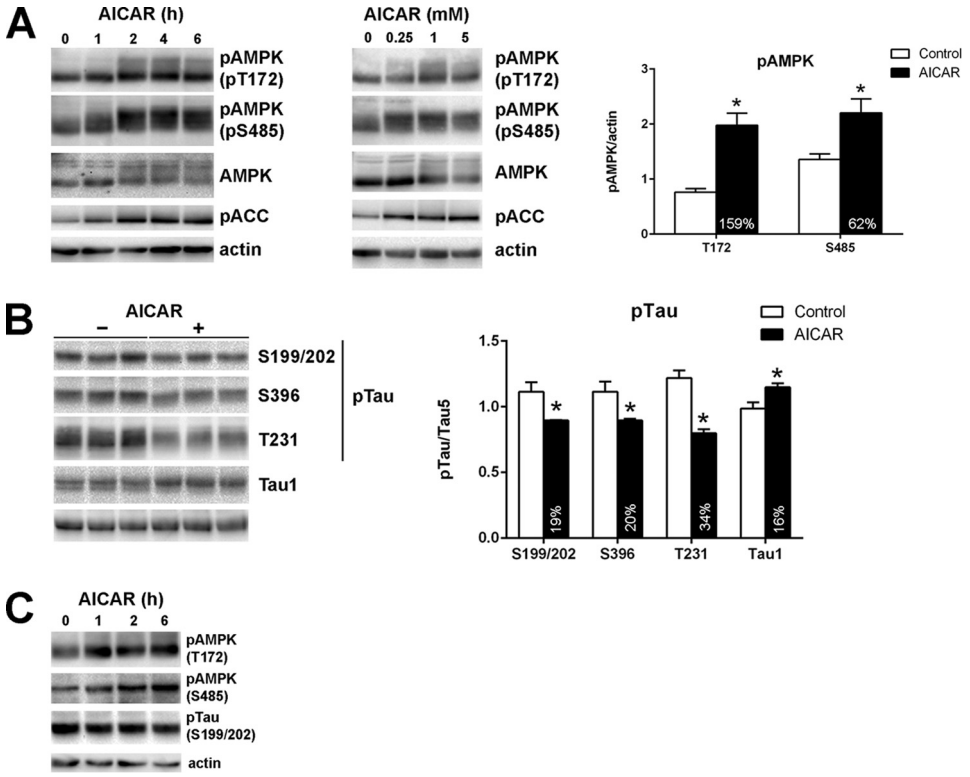

FIGURE 3. **AICAR treatment increases AMPK phosphorylation and decreases Tau phosphorylation.** *A*, HK-532 cells were differentiated for 1 week and treated with 1 mM AICAR for 0–6 h (*left panel*) or increasing concentrations of AICAR for 2 h (*middle panel*). The results of AMPK phosphorylation with 1 mM AICAR for 2 h treatment are shown in the graph on the *right*. *B*, HK-532 cells were treated with 1 mM AICAR for 2 h, and Tau phosphorylation was examined. *C*, primary rat embryonic cortical neurons were treated with 1 mM AICAR for 0–6 h. Cell lysates were prepared in radioimmune precipitation assay buffer and immunoblotted with the indicated antibodies, Anti-actin immunoblots demonstrate the equal protein loading. *, $p < 0.05$ by *t* test.

AMPK activity (32), and it is also reported that AMPK can activate PI3-K/Akt pathway (45, 46). Here, we demonstrate that AICAR treatment of HK-532 cells also increases Akt phosphorylation, whereas insulin pretreatment significantly increased AICAR-mediated Akt phosphorylation (Fig. 5*B*). AICAR treatment did not increase ERK phosphorylation with or without insulin pretreatment (Fig. 5*B*). We previously reported that prevention of Akt hyperactivation restored insulin responsiveness and reversed IR in DRG and cortical neurons (43, 44). Similarly, treatment of HK-532 cells with insulin along with LY294002 to inhibit the hyperactivation of Akt prevented the overphosphorylation of AMPK$^{Ser-485}$ by AICAR (Fig. 5, *C* and *D*, *panel b*). As expected, AMPK$^{Thr-172}$ phosphorylation was not affected by insulin or LY294002 treatment (Fig. 5, *C* and *D*, *panel a*). LY294002 treatment also restored AICAR-mediated dephosphorylation of Tau (Fig. 5, *C* and *D*, *panel c*). Treatment with the MAPK inhibitor, U0126, had no effect on AMPK$^{Ser-485}$ or Tau phosphorylation (Fig. 5*C*). These results strongly suggest that hyperactivation of Akt increases AMPK$^{Ser-485}$ phosphorylation and ultimately leads to the inhibition of AMPK-mediated dephosphorylation of Tau.

Finally, to confirm the specific contribution of AMPK$^{Ser-485}$ phosphorylation, we transfected HK-532 cells with lentiviral vectors expressing nonphosphorylatable mutants of AMPK$^{Ser-485}$, AMPK S485A. Transfection of AMPK S485A decreased basal as well as AICAR-induced AMPK$^{Ser-485}$ phosphorylation and slightly increased AMPK$^{Thr-172}$ phosphorylation (Fig. 6*A*). AMPK S485A transfection suppressed AMPK$^{Ser-485}$ hyperphosphorylation after insulin pretreatment (Fig. 6*B*). Tau phosphorylation levels correlated well with the reduced AMPK$^{Ser-485}$ phosphorylation, and more importantly, AMPK S485A transfection restored the ability of AICAR to reduce Tau phosphorylation after insulin pretreatment (Fig. 6*C*). Stable transfection of S485A, but not S485D, mutant also reversed the inhibitor effect of IR on AICAR-induced Tau phosphorylation (Fig. 6, *D* and *E*). These results emphasize the direct and important role of Ser-485 in AMPK-mediated Tau phosphorylation.

Discussion

It is now well established that MetS, including obesity and diabetes, is a risk factor for AD (5, 6). IR is at the core of MetS, and studies suggest that IR has an important role for the development/acceleration of AD and further emphasize the need for precise regulation of energy expenditure (6, 7). There is significant gap in our knowledge, however, about the molecular link between IR and increased risk of AD. Considering the important role of AMPK in energy metabolism, we can naturally speculate that it is the crucial link between IR and AD. In the current study, we report that the activation of AMPK by AICAR resulted in Tau dephosphorylation and that chronic insulin treatment prevented AICAR-induced Tau dephosphorylation. Furthermore, we demonstrated for the first time that chronic insulin treatment specifically increased AICAR-induced AMPK$^{Ser-485}$ phosphorylation, consistent with what is observed in the brains of the diabetes and obesity mouse models, and preventing hyperactivation of Akt during chronic insulin

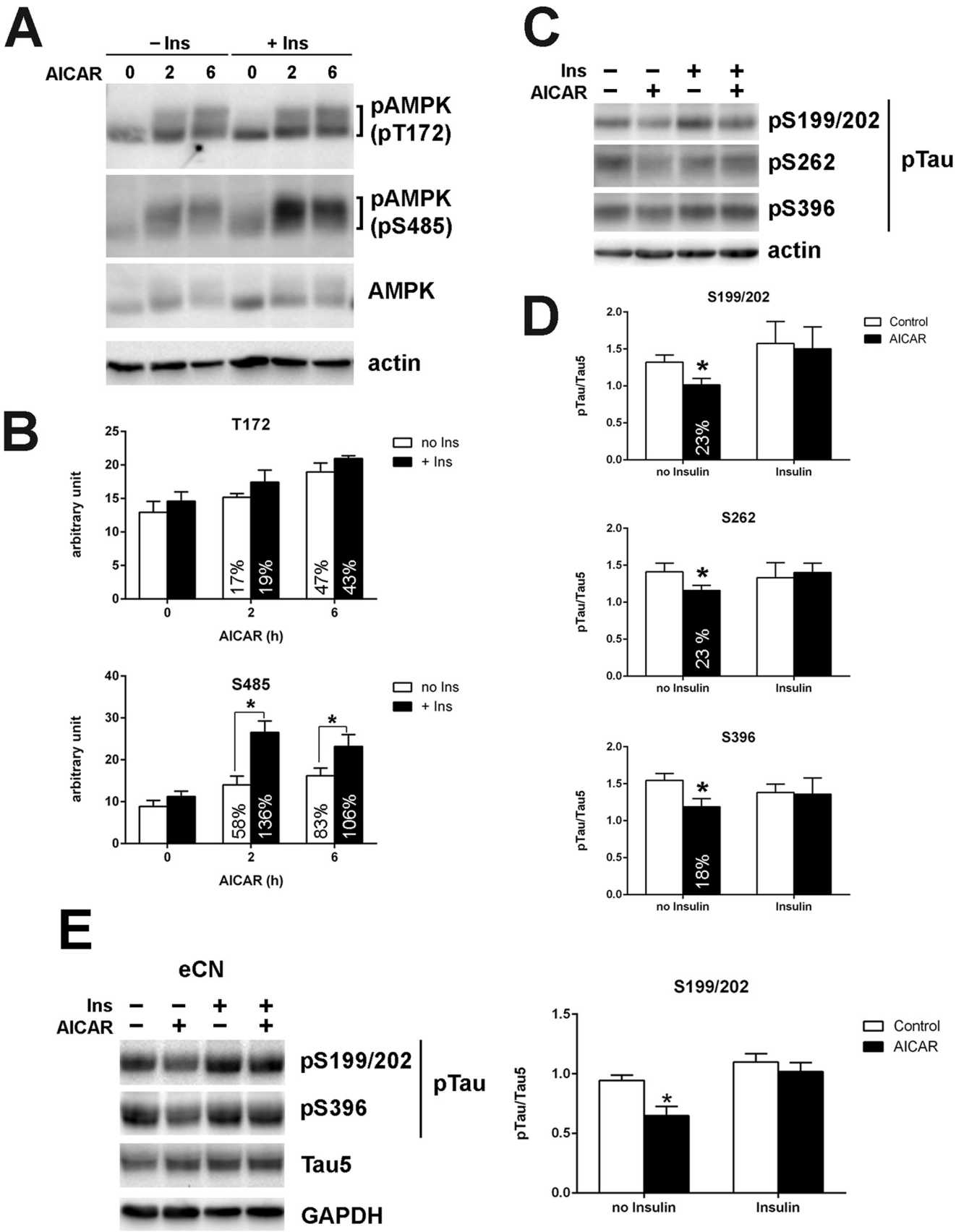
A
– Ins
+ Ins
AICAR 0 2 6 0 2 6
pAMPK (pT172)
pAMPK (pS485)
AMPK
actin
B
T172
arbitrary unit
no Ins
+ Ins
17%
19%
47%
43%
AICAR (h)
S485
58%
136%
83%
106%
C
Ins – – + +
AICAR – + – +
pS199/202
pS262
pS396
actin
pTau
D
S199/202
pTau/Tau5
Control
AICAR
23%
no Insulin
Insulin
S262
23 %
S396
18%
E
eCN
pS199/202
pS396
Tau5
GAPDH
pTau
S199/202

treatment prevented the overphosphorylation of Ser-485 and subsequently restored the ability of AMPK to reduce Tau phosphorylation. Together, these results emphasize the important role of AMPK$^{Ser\text{-}485}$ in AMPK regulation of Tau phosphorylation, especially in IR.

Given that most of the studies of AMPK are focused on peripheral tissues, there is very limited knowledge about the regulation AMPK in brain regions other than the hypothalamus (47, 48). Our results from mouse brains demonstrate that MetS induces a specific increase in AMPK$^{Ser\text{-}485}$ phosphorylation in the cortices of both db/db and obese mice. We also observed increased Akt phosphorylation in these brains caused by IR (44), suggesting that increased Akt may contribute to the increased AMPK$^{Ser\text{-}485}$ phosphorylation (31, 32). In a very recent report, Arnold *et al.* (49) demonstrated for the first time that AMPK phosphorylation is increased in the brain of HFD-fed mice; however, their results only report AMPK$^{Thr\text{-}172}$ phosphorylation,[3] which showed no changes in our study. This discrepancy may arise from apparent differences in the feeding scheme of the HFD between our study and theirs regarding the fat content (54% *versus* 60%), duration of feeding (24 weeks *versus* 17 days), and when the diet was initiated (4 weeks *versus* 8 weeks). Similarly, in another report, intracerebroventricular injection of streptozotocin decreased AMPK phosphorylation and increased Tau phosphorylation, both of which were reversed by AICAR administration (50). Because there are very few studies about AMPK in the brain, more research is required to obtain consistent results.

The exact contribution of AMPK to AD pathology is still controversial, with the results supporting both beneficial and detrimental effects (20, 24–29). Our results demonstrate a causal relationship between increased AMPK$^{Ser\text{-}485}$ and Tau phosphorylation in db/db and obese mouse brains. Our current study does not clearly describe whether Tau phosphorylation is regulated directly by AMPK, especially AMPK$^{Ser\text{-}485}$ phosphorylation, or through other kinases. However, the close correlation between AMPK and Tau phosphorylation observed *in vivo* along with our *in vitro* results strongly suggest the important contribution of AMPK$^{Ser\text{-}485}$ on Tau phosphorylation. Most of the studies about the connection between AMPK and AD pathology focus only on AMPK$^{Thr\text{-}172}$ phosphorylation. It is possible that the status of AMPK$^{Ser\text{-}485}$ phosphorylation (which was not examined in previous reports) might have resulted in the contradictory findings.

The important role of AMPK$^{Ser\text{-}485}$ phosphorylation on Tau phosphorylation is supported by our *in vitro* results. In agreement with published reports (26, 27), we show that activation of AMPK by AICAR reduced Tau phosphorylation, whereas induction of IR correlates with a specific increase in AMPK$^{Ser\text{-}485}$ phosphorylation and prevents AICAR-induced Tau dephosphorylation. However, our results demonstrating that increased AMPK$^{Ser\text{-}485}$ phosphorylation during IR did not affect AMPK$^{Thr\text{-}172}$ phosphorylation conflict with previous reports demonstrating that increases in AMPK$^{Ser\text{-}485}$ phosphorylation are generally accompanied by decreased AMPK$^{Thr\text{-}172}$ phosphorylation (31, 32, 51). This may possibly be due to the relatively small increase in AMPK$^{Ser\text{-}485}$ phosphorylation observed during IR, or it could be that AMPK$^{Ser\text{-}485}$-mediated regulation of Tau phosphorylation is independent of AMPK$^{Thr\text{-}172}$ phosphorylation. Thus, the precise role of AMPK on Tau phosphorylation is still controversial and likely depends on the context of the experiments.

AMPK$^{Thr\text{-}172}$ is phosphorylated by LKB1 or Ca^{2+}/calmodulin-dependent protein kinase kinase β (21, 30), whereas AMPK$^{Ser\text{-}485}$ is phosphorylated by Akt (31, 32). Our *in vitro* data further demonstrate that AMPK reciprocally increases the phosphorylation and activation of Akt. Interestingly, AMPK activation during IR significantly increased Akt phosphorylation, correlating well with the specific increase of AMPK$^{Ser\text{-}485}$ phosphorylation. Although some studies suggest cooperative interactions between AMPK and Akt activation (45, 46), we believe, at least in our system, that AICAR-mediated Akt activation serves as a negative feedback regulator that limits AMPK activity. Indeed, we observe that AMPK$^{Thr\text{-}172}$ phosphorylation returns to basal levels after long term (>8 h) AICAR treatment (data not shown). Thus, IR induces overactivation of Akt and a subsequent increase in AMPK$^{Ser\text{-}485}$ phosphorylation, which results in the disruption of AMPK signaling.

In the current study, we further demonstrate that Akt hyperphosphorylation by AMPK in IR results in inhibition of AMPK-mediated Tau dephosphorylation and that AMPK$^{Ser\text{-}485}$ phosphorylation has a direct role in Tau phosphorylation using two Ser-485 phosphorylation-resistant AMPK mutant constructs. There are reports for both increased (28, 29) and decreased (25–27, 50) Tau phosphorylation by AMPK activation; however, none of the studies examined the role of AMPK$^{Ser\text{-}485}$ phosphorylation, and very few examined the connection between IR and AMPK in the brain (49, 50). Of note, insulin antagonizes AMPK activation by increased phosphorylation of AMPK$^{Ser\text{-}485}$ (31, 52); therefore, we believe that IR overactivates Akt, resulting in increased AMPK$^{Ser\text{-}485}$ phosphorylation and subsequent inhibition of Tau dephosphorylation.

Our results are summarized in the model (Fig. 7). In normal conditions, AMPK regulates Tau phosphorylation through balanced phosphorylation of Thr-172 and Ser-485. AMPK-mediated Akt phosphorylation may act as a negative feedback mechanism for a precise regulation of AMPK activity. In the MetS status, IR induces impaired insulin/Akt signaling, with supporting data for not only reduced Akt acti-

[3] S. E. Arnold, I. Lucki, B. R. Brookshire, G. C. Carlson, C. A. Browne, H. Kazi, S. Bang, B. R. Choi, Y. Chen, M. F. McMullen, and S. F. Kim, personal communication.

FIGURE 4. **Insulin pretreatment specifically increases AMPK$^{Ser\text{-}485}$ phosphorylation and prevents AICAR-induced Tau dephosphorylation.** *A*, HK-532 cells were treated without (− *Ins*) or with (+ *Ins*) 50 nM insulin overnight and then treated with 1 mM AICAR for 0, 2, or 6 h. *B*, when the cells were pretreated with 50 nM insulin overnight, AICAR treatment specifically increased AMPK$^{Ser\text{-}485}$ phosphorylation. *, $p < 0.05$ compared with Ser-485 phosphorylation without insulin pretreatment at same time point. *C*, the cells were treated without or with 50 nM insulin overnight and then treated with 1 mM AICAR for 2 h. Insulin pretreatment prevented AICAR-induced Tau dephosphorylation. *D*, densitometric analysis of phosphorylated Tau (*pTau*). *E*, insulin pretreatment also prevented AICAR-induced Tau dephosphorylation in embryonic rat primary cortical neurons (*eCN*). *, $p < 0.05$ compared with control by *t* test.

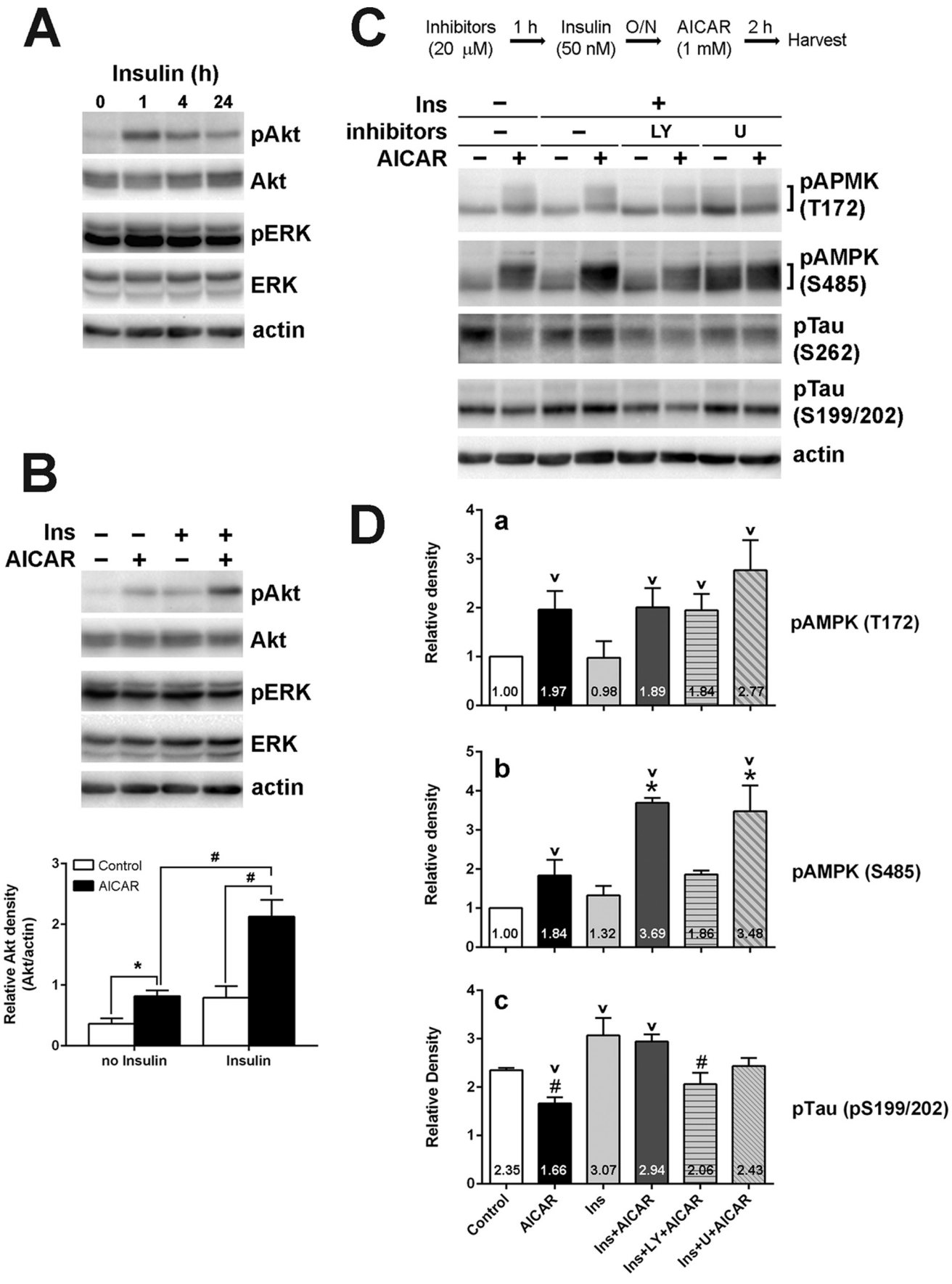
A
Insulin (h)
0 1 4 24
pAkt
Akt
pERK
ERK
actin
B
Ins – – + +
AICAR – + – +
pAkt
Akt
pERK
ERK
actin
Control
AICAR
Relative Akt density (Akt/actin)
no Insulin
Insulin
C
Inhibitors (20 μM) 1 h Insulin (50 nM) O/N AICAR (1 mM) 2 h Harvest
Ins – +
inhibitors – – LY U
AICAR – + – + – + – +
pAPMK (T172)
pAMPK (S485)
pTau (S262)
pTau (S199/202)
actin
D
a
Relative density
1.00 1.97 0.98 1.89 1.84 2.77
pAMPK (T172)
b
Relative density
1.00 1.84 1.32 3.69 1.86 3.48
pAMPK (S485)
c
Relative Density
2.35 1.66 3.07 2.94 2.06 2.43
pTau (pS199/202)
Control
AICAR
Ins
Ins+AICAR
Ins+LY+AICAR
Ins+U+AICAR

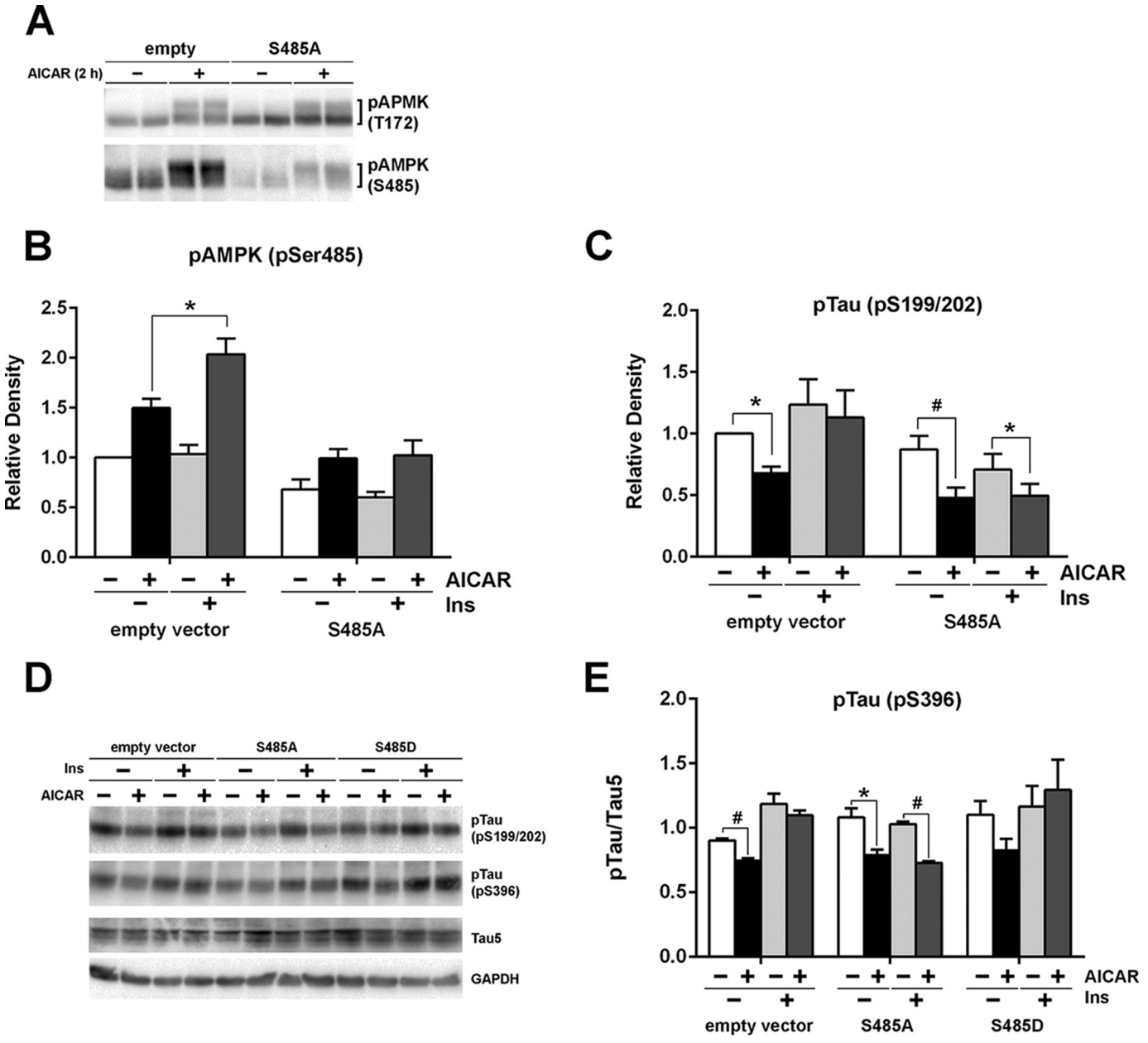

FIGURE 6. **Preventing AMPK$^{Ser-485}$ hyperphosphorylation by mutating Ser-485 restored AICAR-induced Tau dephosphorylation by insulin pretreatment.** *A*, HK-532 cell were infected with a lentiviral vector expressing S485A AMPK mutants or control for 5 days. S485A mutant transfection reduced both basal and AICAR-induced Ser-485 phosphorylation by AICAR. The cells were treated without or with 50 nM insulin overnight and then treated with 1 mM AICAR for 2 h. *B* and *C*, cell lysates were examined for AMPK (*B*) and Tau (*C*) phosphorylation. *D*, HK-532 cells were transfected with S485A or S485D AMPK mutant, and the stable clones were selected by puromycin. AICAR-induced Tau dephosphorylation was examined after without or with 50 nM overnight insulin pretreatment. *E*, densitometry of the result of stable AMPK mutant transfection. *, $p < 0.05$; #, $p < 0.005$.

vation but also instances of chronic overactivation of Akt (43, 44). Overactivation of Akt in IR subsequently leads to the hyperphosphorylation of AMPK$^{Ser-485}$. These changes result in the elevated phosphorylation of Tau. It is not clear from our study whether AMPK$^{Ser-485}$ affects Tau phosphorylation through inhibitory action on AMPK$^{Thr-172}$ or direct independent action on Tau. Our results suggest for the first time a possible contribution of AMPK$^{Ser-485}$ phosphorylation toward the increased risk of AD in IR associated with diabetes and obesity. Furthermore, this study supports a new

FIGURE 5. **Hyperactivation of Akt by insulin pretreatment is responsible for the increased AMPK$^{Ser-485}$ phosphorylation in HK-532 cells.** *A*, HK-532 cells were treated with 20 nM insulin and Akt, and ERK phosphorylation was examined. *B*, HK-532 cells were incubated overnight without or with 50 nM insulin (*Ins*) and then treated with 1 mM AICAR for 2 h. Insulin pretreatment significantly increased AICAR induced Akt phosphorylation. *, $p < 0.05$; #, $p < 0.01$ by *t* test. *C*, the cells were incubated with insulin along with 20 μM LY294002 (*LY*) or U0126 (*U*) overnight. The cells were washed and treated with 1 mM AICAR for 2 h. *D*, inhibiting Akt overactivation during insulin pretreatment by LY294002 prevented AMPK$^{Ser-485}$ hyperphosphorylation (*b*) and restored AICAR-induced Tau dephosphorylation. (*c*) but did not affect AMPK$^{Thr-172}$ phosphorylation (*a*). *, $p < 0.05$ compared with insulin + LY294002 + AICAR; #, $p < 0.05$ compared with insulin or insulin + AICAR; ^{v}, $p < 0.05$ compared with control.

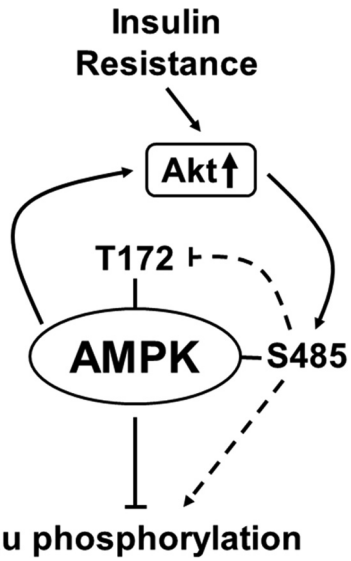

FIGURE 7. **Model summarizing our study.** IR induces chronic overactivation of Akt and subsequent hyperphosphorylation of AMPK$^{Ser-485}$. These changes result in the elevated phosphorylation of Tau and may contribute the progression of AD.

direction of investigation into the role of AMPK in AD and possibly other neurodegenerative diseases as well.

Author Contributions—B. K. designed and coordinated the study and wrote the paper. C. F.-G. designed and constructed vectors for expression of mutant AMPK and analyzed the mutant phenotypes on Fig 6. C. P. and C. B. provided technical assistance and preparation of the figures. E. L. F. revised the article and provided critical feedback.

References

1. Querfurth, H. W., and LaFerla, F. M. (2010) Alzheimer's disease. *N. Engl. J. Med.* **362,** 329–344
2. Johnson, G. V., and Stoothoff, W. H. (2004) Tau phosphorylation in neuronal cell function and dysfunction. *J. Cell Sci.* **117,** 5721–5729
3. Martin, L., Latypova, X., and Terro, F. (2011) Post-translational modifications of Tau protein: implications for Alzheimer's disease. *Neurochem. Int.* **58,** 458–471
4. Duvnjak, L., and Duvnjak, M. (2009) The metabolic syndrome: an ongoing story. *J. Physiol. Pharmacol.* **60,** 19–24
5. Kim, B., and Feldman, E. L. (2012) Insulin resistance in the nervous system. *Trends Endocrinol. Metab.* **23,** 133–141
6. Frisardi, V., Solfrizzi, V., Capurso, C., Imbimbo, B. P., Vendemiale, G., Seripa, D., Pilotto, A., and Panza, F. (2010) Is insulin resistant brain state a central feature of the metabolic-cognitive syndrome? *J. Alzheimers Dis.* **21,** 57–63
7. Lester-Coll, N., Rivera, E. J., Soscia, S. J., Doiron, K., Wands, J. R., and de la Monte, S. M. (2006) Intracerebral streptozotocin model of type 3 diabetes: relevance to sporadic Alzheimer's disease. *J. Alzheimers Dis.* **9,** 13–33
8. Luchsinger, J. A., Tang, M. X., Shea, S., and Mayeux, R. (2002) Caloric intake and the risk of Alzheimer disease. *Arch. Neurol.* **59,** 1258–1263
9. Ott, A., Stolk, R. P., van Harskamp, F., Pols, H. A., Hofman, A., and Breteler, M. M. (1999) Diabetes mellitus and the risk of dementia: the Rotterdam Study. *Neurology* **53,** 1937–1942
10. Peila, R., Rodriguez, B. L., and Launer, L. J. (2002) Type 2 diabetes, APOE gene, and the risk for dementia and related pathologies: the Honolulu-Asia Aging Study. *Diabetes* **51,** 1256–1262
11. Biessels, G. J., and Kappelle, L. J. (2005) Increased risk of Alzheimer's disease in type II diabetes: insulin resistance of the brain or insulin-induced amyloid pathology? *Biochem. Soc. Trans.* **33,** 1041–1044
12. Cox, D. J., Kovatchev, B. P., Gonder-Frederick, L. A., Summers, K. H., McCall, A., Grimm, K. J., and Clarke, W. L. (2005) Relationships between hyperglycemia and cognitive performance among adults with type 1 and type 2 diabetes. *Diabetes Care* **28,** 71–77
13. Brands, A. M., Biessels, G. J., de Haan, E. H., Kappelle, L. J., and Kessels, R. P. (2005) The effects of type 1 diabetes on cognitive performance: a meta-analysis. *Diabetes Care* **28,** 726–735
14. Janson, J., Laedtke, T., Parisi, J. E., O'Brien, P., Petersen, R. C., and Butler, P. C. (2004) Increased risk of type 2 diabetes in Alzheimer disease. *Diabetes* **53,** 474–481
15. de la Monte, S. M. (2009) Insulin resistance and Alzheimer's disease. *BMB Rep.* **42,** 475–481
16. Hölscher, C. (2011) Diabetes as a risk factor for Alzheimer's disease: insulin signalling impairment in the brain as an alternative model of Alzheimer's disease. *Biochem. Soc. Trans.* **39,** 891–897
17. Galindo, M. F., Ikuta, I., Zhu, X., Casadesus, G., and Jordán, J. (2010) Mitochondrial biology in Alzheimer's disease pathogenesis. *J. Neurochem.* **114,** 933–945
18. Wang, X., Su, B., Lee, H. G., Li, X., Perry, G., Smith, M. A., and Zhu, X. (2009) Impaired balance of mitochondrial fission and fusion in Alzheimer's disease. *J. Neurosci.* **29,** 9090–9103
19. Carlsson, C. M. (2010) Type 2 diabetes mellitus, dyslipidemia, and Alzheimer's disease. *J. Alzheimers Dis.* **20,** 711–722
20. Salminen, A., Kaarniranta, K., Haapasalo, A., Soininen, H., and Hiltunen, M. (2011) AMP-activated protein kinase: a potential player in Alzheimer's disease. *J. Neurochem.* **118,** 460–474
21. Cai, Z., Yan, L. J., Li, K., Quazi, S. H., and Zhao, B. (2012) Roles of AMP-activated protein kinase in Alzheimer's disease. *Neuromolecular Med.* **14,** 1–14
22. Carling, D., Mayer, F. V., Sanders, M. J., and Gamblin, S. J. (2011) AMP-activated protein kinase: nature's energy sensor. *Nat. Chem. Biol.* **7,** 512–518
23. Mihaylova, M. M., and Shaw, R. J. (2011) The AMPK signalling pathway coordinates cell growth, autophagy and metabolism. *Nat. Cell Biol.* **13,** 1016–1023
24. Won, J. S., Im, Y. B., Kim, J., Singh, A. K., and Singh, I. (2010) Involvement of AMP-activated-protein-kinase (AMPK) in neuronal amyloidogenesis. *Biochem. Biophys. Res. Commun.* **399,** 487–491
25. Vingtdeux, V., Giliberto, L., Zhao, H., Chandakkar, P., Wu, Q., Simon, J. E., Janle, E. M., Lobo, J., Ferruzzi, M. G., Davies, P., and Marambaud, P. (2010) AMP-activated protein kinase signaling activation by resveratrol modulates amyloid-beta peptide metabolism. *J. Biol. Chem.* **285,** 9100–9113
26. Greco, S. J., Sarkar, S., Johnston, J. M., and Tezapsidis, N. (2009) Leptin regulates Tau phosphorylation and amyloid through AMPK in neuronal cells. *Biochem. Biophys. Res. Commun.* **380,** 98–104
27. Greco, S. J., Hamzelou, A., Johnston, J. M., Smith, M. A., Ashford, J. W., and Tezapsidis, N. (2011) Leptin boosts cellular metabolism by activating AMPK and the sirtuins to reduce Tau phosphorylation and beta-amyloid in neurons. *Biochem. Biophys. Res. Commun.* **414,** 170–174
28. Thornton, C., Bright, N. J., Sastre, M., Muckett, P. J., and Carling, D. (2011) AMP-activated protein kinase (AMPK) is a Tau kinase, activated in response to amyloid beta-peptide exposure. *Biochem. J.* **434,** 503–512
29. Vingtdeux, V., Davies, P., Dickson, D. W., and Marambaud, P. (2011) AMPK is abnormally activated in tangle- and pre-tangle-bearing neurons in Alzheimer's disease and other tauopathies. *Acta Neuropathol.* **121,** 337–349
30. Carling, D., Sanders, M. J., and Woods, A. (2008) The regulation of AMP-activated protein kinase by upstream kinases. *Int. J. Obes.* (*Lond.*) **32,** S55–S59
31. Horman, S., Vertommen, D., Heath, R., Neumann, D., Mouton, V., Woods, A., Schlattner, U., Wallimann, T., Carling, D., Hue, L., and Rider, M. H. (2006) Insulin antagonizes ischemia-induced Thr^{172} phosphorylation of AMP-activated protein kinase α-subunits in heart via hierarchical phosphorylation of Ser$^{485/491}$. *J. Biol. Chem.* **281,** 5335–5340
32. Ning, J., Xi, G., and Clemmons, D. R. (2011) Suppression of AMPK activation via S485 phosphorylation by IGF-I during hyperglycemia is mediated by AKT activation in vascular smooth muscle cells. *Endocrinology* **152,** 3143–3154

33. Leinninger, G. M., Backus, C., Sastry, A. M., Yi, Y. B., Wang, C. W., and Feldman, E. L. (2006) Mitochondria in DRG neurons undergo hyperglycemic mediated injury through Bim, Bax and the fission protein Drp1. *Neurobiol. Dis.* **23,** 11–22
34. Vincent, A. M., McLean, L. L., Backus, C., and Feldman, E. L. (2005) Short-term hyperglycemia produces oxidative damage and apoptosis in neurons. *FASEB J.* **19,** 638–640
35. Kim, B., Backus, C., Oh, S., and Feldman, E. L. (2013) Hyperglycemia-induced Tau cleavage in vitro and in vivo: a possible link between diabetes and Alzheimer's disease. *J. Alzheimers Dis.* **34,** 727–739
36. Kim, B., Backus, C., Oh, S., Hayes, J. M., and Feldman, E. L. (2009) Increased Tau phosphorylation and cleavage in mouse models of type 1 and type 2 diabetes. *Endocrinology* **150,** 5294–5301
37. Watcho, P., Stavniichuk, R., Ribnicky, D. M., Raskin, I., and Obrosova, I. G. (2010) High-fat diet-induced neuropathy of prediabetes and obesity: effect of PMI-5011, an ethanolic extract of Artemisia dracunculus L. *Mediators Inflamm.* **2010,** 268547
38. Obrosova, I. G., Ilnytska, O., Lyzogubov, V. V., Pavlov, I. A., Mashtalir, N., Nadler, J. L., and Drel, V. R. (2007) High-fat diet induced neuropathy of pre-diabetes and obesity: effects of "healthy" diet and aldose reductase inhibition. *Diabetes* **56,** 2598–2608
39. Ahrén, J., Ahrén, B., and Wierup, N. (2010) Increased beta-cell volume in mice fed a high-fat diet: a dynamic study over 12 months. *Islets* **2,** 353–356
40. Copps, K. D., and White, M. F. (2012) Regulation of insulin sensitivity by serine/threonine phosphorylation of insulin receptor substrate proteins IRS1 and IRS2. *Diabetologia* **55,** 2565–2582
41. Ha, J., Daniel, S., Broyles, S. S., and Kim, K. H. (1994) Critical phosphorylation sites for acetyl-CoA carboxylase activity. *J. Biol. Chem.* **269,** 22162–22168
42. Szendrei, G. I., Lee, V. M., and Otvos, L., Jr. (1993) Recognition of the minimal epitope of monoclonal antibody Tau-1 depends upon the presence of a phosphate group but not its location. *J. Neurosci. Res.* **34,** 243–249
43. Kim, B., McLean, L. L., Philip, S. S., and Feldman, E. L. (2011) Hyperinsulinemia induces insulin resistance in dorsal root ganglion neurons. *Endocrinology* **152,** 3638–3647
44. Kim, B., Sullivan, K. A., Backus, C., and Feldman, E. L. (2011) Cortical neurons develop insulin resistance and blunted Akt signaling: a potential mechanism contributing to enhanced ischemic injury in diabetes. *Antioxid. Redox. Signal.* **14,** 1829–1839
45. Kimura, T., Tomura, H., Sato, K., Ito, M., Matsuoka, I., Im, D. S., Kuwabara, A., Mogi, C., Itoh, H., Kurose, H., Murakami, M., and Okajima, F. (2010) Mechanism and role of high density lipoprotein-induced activation of AMP-activated protein kinase in endothelial cells. *J. Biol. Chem.* **285,** 4387–4397
46. Jessen, N., Pold, R., Buhl, E. S., Jensen, L. S., Schmitz, O., and Lund, S. (2003) Effects of AICAR and exercise on insulin-stimulated glucose uptake, signaling, and GLUT-4 content in rat muscles. *J. Appl. Physiol.* **94,** 1373–1379
47. Dagon, Y., Hur, E., Zheng, B., Wellenstein, K., Cantley, L. C., and Kahn, B. B. (2012) p70S6 kinase phosphorylates AMPK on serine 491 to mediate leptin's effect on food intake. *Cell Metab.* **16,** 104–112
48. Xue, B., and Kahn, B. B. (2006) AMPK integrates nutrient and hormonal signals to regulate food intake and energy balance through effects in the hypothalamus and peripheral tissues. *J. Physiol.* **574,** 73–83
49. Arnold, S. E., Lucki, I., Brookshire, B. R., Carlson, G. C., Browne, C. A., Kazi, H., Bang, S., Choi, B. R., Chen, Y., McMullen, M. F., and Kim, S. F. (2014) High fat diet produces brain insulin resistance, synaptodendritic abnormalities and altered behavior in mice. *Neurobiol. Dis.* **67,** 79–87
50. Du, L. L., Chai, D. M., Zhao, L. N., Li, X. H., Zhang, F. C., Zhang, H. B., Liu, L. B., Wu, K., Liu, R., Wang, J. Z., and Zhou, X. W. (2015) AMPK activation ameliorates Alzheimer's disease-like pathology and spatial memory impairment in a streptozotocin-induced Alzheimer's disease model in rats. *J. Alzheimers Dis.* **43,** 775–784
51. Hurley, R. L., Barré, L. K., Wood, S. D., Anderson, K. A., Kemp, B. E., Means, A. R., and Witters, L. A. (2006) Regulation of AMP-activated protein kinase by multisite phosphorylation in response to agents that elevate cellular cAMP. *J. Biol. Chem.* **281,** 36662–36672
52. Kovacic, S., Soltys, C. L., Barr, A. J., Shiojima, I., Walsh, K., and Dyck, J. R. (2003) Akt activity negatively regulates phosphorylation of AMP-activated protein kinase in the heart. *J. Biol. Chem.* **278,** 39422–39427